



UvA-DARE (Digital Academic Repository)

Glow with the flow: Quantifying blood flow and photoluminescence signal in biological tissue

Nadort, A.

Publication date

2015

Document Version

Final published version

[Link to publication](#)

Citation for published version (APA):

Nadort, A. (2015). *Glow with the flow: Quantifying blood flow and photoluminescence signal in biological tissue*. [Thesis, fully internal, Universiteit van Amsterdam].

General rights

It is not permitted to download or to forward/distribute the text or part of it without the consent of the author(s) and/or copyright holder(s), other than for strictly personal, individual use, unless the work is under an open content license (like Creative Commons).

Disclaimer/Complaints regulations

If you believe that digital publication of certain material infringes any of your rights or (privacy) interests, please let the Library know, stating your reasons. In case of a legitimate complaint, the Library will make the material inaccessible and/or remove it from the website. Please Ask the Library: <https://uba.uva.nl/en/contact>, or a letter to: Library of the University of Amsterdam, Secretariat, P.O. Box 19185, 1000 GD Amsterdam, The Netherlands. You will be contacted as soon as possible.



2

LASER SPECKLE CONTRAST IMAGING

ABSTRACT Dynamic light scattering techniques obtain information about the medium of interest by measuring the intensity fluctuations in dynamically scattered coherent light. The intensity fluctuations relate to the medium dynamics. Laser speckle contrast imaging, laser Doppler flowmetry and diffusing wave spectroscopy make use of this principle to obtain information about tissue perfusion. In this chapter the techniques are introduced and in particular the theoretical background of laser speckle contrast imaging is given, followed by the identification of the essential aspects that need further investigation in order to enable quantitative blood flow velocity measurements.

2.1 INTRODUCTION

The clinical need for a non-invasive microcirculation imaging device at the bedside to monitor the onset and development of critical diseases was illustrated in Chapter 1. Besides non-invasive and compact, other preferential properties are continuous monitoring, and an instantaneous, reproducible and quantitative measurement of microcirculation functionality [1, 2]. Such device could additionally be relevant for internal, surgical and oncologic medicine [3-8]. A clinically approved tool currently used for microcirculation monitoring at the intensive care unit (ICU) is the sidestream dark field (SDF) microscope. SDF videos contain a high level of detail to determine the relevant parameters such as vessel density and geometry; proportion of perfused vessels and microcirculatory heterogeneity [9]. However, the image analysis requires user-interaction, limiting its use at the bedside. In addition, accurate flow measurements require high-contrast images showing red blood cells (RBCs) and plasma gaps [10]. Fast flowing, out of focus, or fully RBC-filled vessels can therefore not be analyzed. An alternative method for measuring flow is based on the dynamical properties of scattered light, as introduced in Chapter 1. Techniques based on this approach do not depend on the aforementioned image properties and their flow sensitivity is based on different principles. In the next section their mechanisms and prospective as favoured flowmetry techniques are discussed.

2.2 DYNAMIC LIGHT SCATTERING TECHNIQUES TO MEASURE BLOOD FLOW

The notion that phase shifts in dynamically scattered coherent light give rise to measurable intensity fluctuations was discovered soon after the launch of the laser in 1960 [11, 12]. The intensity fluctuations are caused by the constructive and destructive interference of the phases of electromagnetic waves (light) and are referred to as 'speckles'. The cause of these phase differences is explained in two ways: by the Doppler-shift in the frequency of the scattered light (Laser Doppler Flowmetry, LDF [13]) and by the path length differences in the reflected light (Laser Speckle Contrast Imaging (LSCI) [14]) and Diffusing Wave Spectroscopy (DWS) [15]). In general, the temporal autocorrelation of the interference pattern of the dynamically scattered light is related to the movement of the scattering particles.

In the case of LDF, the light scattered by moving particles undergoes a frequency shift (Doppler-shift) proportional to the velocity of the moving particle. This frequency shift is very small (10 - 100 kHz) compared to the high frequencies of light (100 THz), therefore the Doppler-shifted light is combined ('mixed') with a non-shifted reference beam resulting in a 'beat' frequency equal to the frequency shift [16]. This is called 'heterodyne' detection. In the case of flowing RBCs, however, not all the cells will have the same velocity but more likely the flow shows a velocity distribution about a mean value. Now the beat frequency will display a spread of frequencies, or a frequency spectrum, centred around the mean frequency shift. In addition, the reflected light from two RBCs with different velocities will also have slightly different Doppler shifts and therefore beat with each other. Thus, all cells together give rise to another self-beating frequency spectrum, centred around zero [17]. This is the homodyne signal detection. Even without a separate reference beam, a heterodyne signal is present from the self-mixing of non-shifted light reflected of static scatterers and the dynamically scattered light. Only for single scattered light for which the

exact angles between blood flow direction, and the incident and the reflected light are known the Doppler shift can be related to the flow velocity. In practice, this has been shown to be very complicated and troublesome [18]. Therefore, most commercial LDF devices do not use a separate reference beam and measure the self-mixing spectrum as a result of dynamic and static scattering in tissue [16]. In LDF the frequency spectrum is generated by recording the temporal intensity fluctuations of the interference pattern by a fast photo-detector and calculating the temporal autocorrelation. By the *Wiener-Khinchine* theorem, the autocorrelation function (ACF) and the power spectral density (PSD) of the intensity (Doppler frequency spectrum) are the Fourier transform of each other [19]. A narrower ACF results in a broader frequency spectrum, and thus a larger Doppler frequency shift implicating a higher velocity. Usually the first moment of the intensity PSD is used as the designated measurement parameter, which is related to the speed of the scatterers and their concentration [20, 21].

The second description for the generation of a fluctuating interference (speckle) pattern is based on phase differences that arise from path length differences between detected photons scattered from different positions within the tissue. When the photons are scattered by moving structures such as flowing RBCs, the optical path lengths will change and the detected speckle pattern fluctuates, referred to as time-varying speckle. Techniques derived from this principle measure these fluctuations either directly (DWS) or indirectly (LSCI). The time-varying speckle and Doppler-induced fluctuations are identical, which is intuitively not obvious. The speckle explanation is based on the superposition of waves of the same optical frequency, whereas in the Doppler explanation the superimposed waves have different frequencies [22]. However, it can be shown mathematically that the two explanations lead to identical equations that link the intensity fluctuations to the tissue dynamics [17, 23] which was later confirmed by simulation and experiment [21, 24].

Similar to LDF, DWS measures the speckle intensity fluctuations of single speckles and calculates the temporal ACF [25]. Because DWS is based on photon correlation in the multiple scattering regime, the illumination source and detector are separated by several centimetres [26]. This results in longer photon paths through tissue and deeper probing of tissue dynamics. Multiple scattering events with dynamic scatterers result in faster decorrelation of the photons. Consequently, speckle decorrelation happens on a shorter timescale and the ACF is measured at high sampling rates. The characteristic timescale for the decay of the ACF is referred to as the decorrelation time τ_c . The tissue dynamics and τ_c are inversely related, making τ_c an important measurement parameter in DWS.

Alternatively, the time-fluctuating speckle pattern can also be imaged as an ensemble of speckles using a camera. It is easy to see that a fluctuating pattern will look blurry in an image when the exposure time is long. The faster the fluctuations, the more blur in the imaged speckle pattern. This is the basic principle of laser speckle flowmetry techniques first introduced by Fercher and Briers [14]. The speckle blur, or speckle contrast, can be quantified mathematically since a blurred pattern will have a low standard deviation in intensity (σ_i) as compared to a sharp pattern, but the mean intensity ($\langle I \rangle$) is unchanged. The speckle contrast K is therefore defined as the ratio $\sigma_i / \langle I \rangle$ and depends on the integration time of the detector and the velocity of the scatterers and is valued between 0

and 1 [27]. Laser speckle flowmetry techniques quantify the speckle contrast to measure or image blood flow and have been named laser speckle contrast analysis (LASCA [27], including the variations tLASCA (temporal) and sLASCA (spatial) [28]), laser speckle imaging (LSI [29, 30]), laser speckle contrast imaging (LSCI [31-34]), speckle-visibility spectroscopy (SVS [35]) and multi-exposure speckle imaging (MESI [36]), amongst others. In this thesis I refer to the technique as Laser Speckle Contrast Imaging - LSCI. As will be mathematically shown in Section 2.4 the contrast depends on the integration of the ACF over the exposure time. The measured quantity K is an indirect measurement of the ACF and relates to tissue dynamics, similar to the LDF and DWS techniques.

2.3 PRACTICAL DIFFERENCES BETWEEN LDF, DWS AND LSCI

The theoretical frameworks of the discussed dynamic light scattering techniques to measure blood flow are highly related. I will therefore summarize the main practical differences between the techniques and their applicability to microcirculation assessment. Techniques based on LDF and DWS measure the temporal autocorrelation in a single speckle directly at high sampling frequencies (\sim kHz) at one measurement point and need fast sampling photodiodes, CMOS cameras or photomultiplier tubes. In addition, in DWS the signal is usually low, which reduces the signal-to-noise ratio and makes detection sensitivity important. This makes the technical requirements of LDF and DWS more complicated compared to LSCI, which quantifies the temporal autocorrelation of speckles integrated over camera exposure times in the millisecond timeframe. For an increased accuracy of LSCI multiple frames and exposure times are desirable, which a standard CCD camera permits. In addition, LSCI is a full-field technique while for LDF scanning of the laser beam (and detector) is needed to obtain an image, making LDF imaging much slower (minutes versus sub-seconds). DWS has a high temporal resolution (single-point measurement), but a very low spatial resolution, compensated by a deep probing of tissue (> 1 cm deep) [26, 37, 38]. For this reason, DWS is not suitable for microcirculation imaging since the dominant decorrelation will be due to the deeper, larger and faster flowing vessels. Spatial resolution and probing depth are often interrelated via the wavelength of light and the distance between the light source and detector. Like DWS, LSCI and LDF operate in the near infrared window (relatively deep tissue penetration) but with shorter source detector separations and are estimated to measure flow at depths of several mm's [18, 39]. The spatial resolution of LSCI and LDF are similar, and depend on the detection and tissue geometry (e.g. numerical aperture (NA) of detection optics, scattering of tissue layers like skin). The spatial resolution of LSCI is slightly further reduced since the speckle contrast is calculated using several spatial speckles, although ergodicity allows the speckle contrast to be measured temporally as well [40, 41]. An overview of the discussed dynamic light scattering techniques, in addition to SDF microscopy, is given in Fig. 2.1.

2.4 LASER SPECKLE CONTRAST IMAGING

The instrumental simplicity of LSCI makes it a favourable candidate for microcirculation monitoring. Since LSCI does not put stringent requirements on the detector, it can easily be combined with the clinical SDF microcirculation imager (Microscan, Microvision Medical Inc. The Netherlands) equipped with a CCD camera. For the results of Chapters 3 and 4

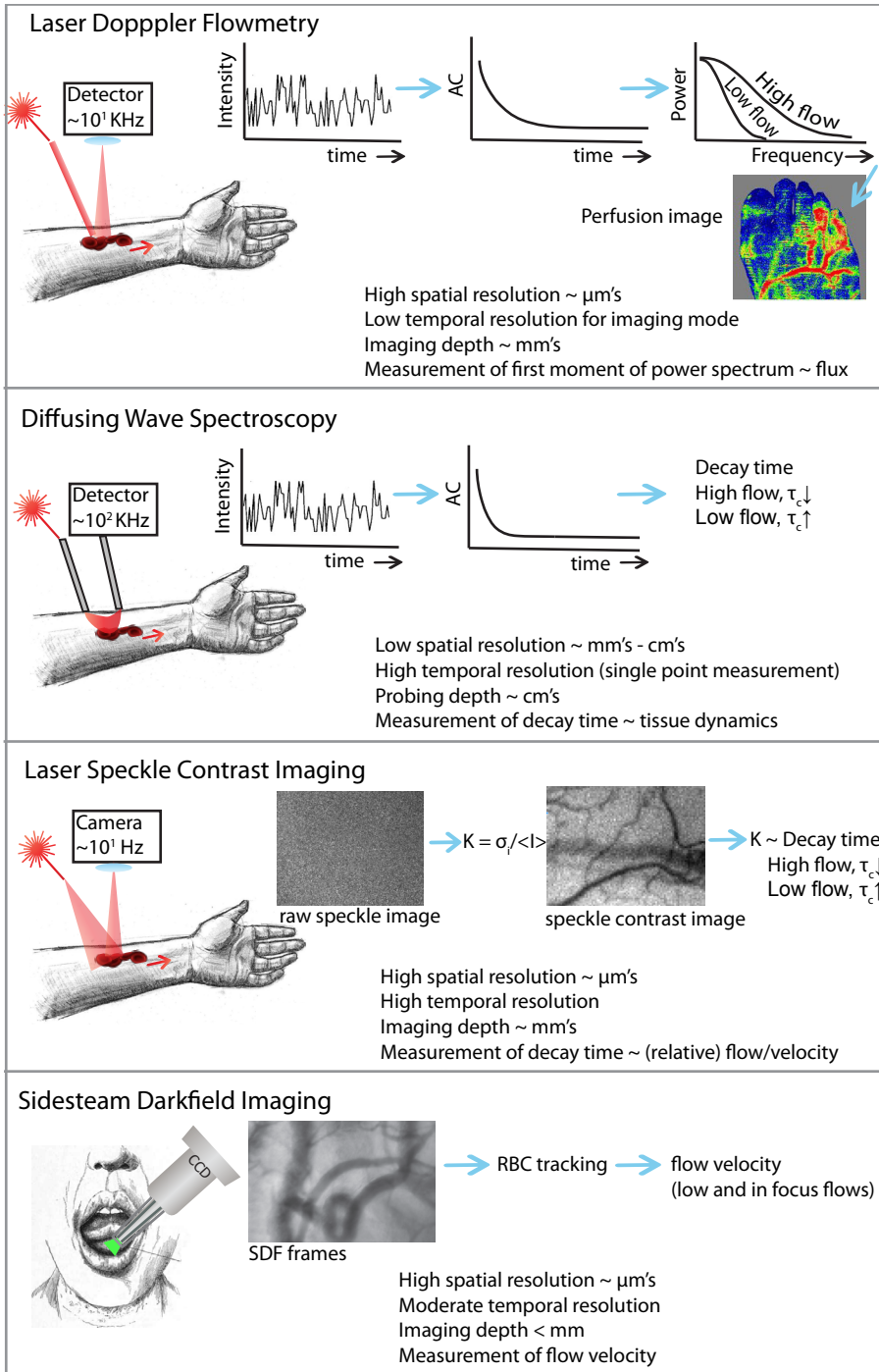


Fig. 2.1. | Schematic overview of blood flow imaging techniques. Arm sketch adapted from Nobges, deviantART, LDF perfusion image adapted from Graduate School of Biomedical Sciences, Hiroshima University

we modified the Microscan for integrated SDF-LSCI microscopy. This allowed for the direct comparison of the measured speckle contrast K and blood flow velocities in the microcirculation measured using SDF. The exact relationship between K and blood flow is a much discussed topic in laser speckle flowmetry. In Chapters 3 and 4 theoretical and experimental contributions to understand this complicated relationship are presented. Below, I start with the mathematical derivation of speckle contrast K from the ACF of the time-varying speckle pattern and introduce the challenges that are facing quantitative laser speckle flowmetry.

Goodman has shown that the spatial statistics of a time-integrated speckle pattern are related to the temporal statistics of speckle fluctuations [19]:

$$\sigma_s^2 = \frac{2}{T} \int_0^T \left(1 - \frac{\tau}{T}\right) C_\tau(\tau) d\tau \quad (2.1)$$

here σ_s^2 is the spatial variance in the speckle pattern, T is the camera exposure time and $C_\tau(\tau)$ is the autocovariance of the temporal speckle intensity. Thus, the variance of the spatial intensity pattern depends on the time integrated autocovariance of the intensity fluctuations. Essentially, LDF and DWS measure the right-hand side of Eq. (2.1) while LSCI measures the left-hand side. $C_\tau(\tau)$ is defined as:

$$C_\tau(\tau) = \left\langle \left\{ I(t) - \langle I \rangle_t \right\} \left\{ I(t + \tau) - \langle I \rangle_t \right\} \right\rangle_t = \langle I(t)I(t + \tau) \rangle_t - \langle I \rangle_t^2 \quad (2.2)$$

Here $I(t)$ is the intensity measured at time t (or $t + \tau$), and $\langle \dots \rangle_t$ is the time average. Assuming ergodicity, we can replace the time average/variance by the ensemble average/variance and vice versa (writing $\langle I \rangle$ and σ_i). Division by $\langle I \rangle^2$ relates Eq. (2.1) to speckle contrast K [14, 19, 35]:

$$K^2 = \frac{\sigma_i^2}{\langle I \rangle^2} = \frac{2}{\langle I \rangle^2 T} \int_0^T \left(1 - \frac{\tau}{T}\right) C_\tau(\tau) d\tau \quad (2.3)$$

Substituting Eq. (2.2) in Eq. (2.3) gives:

$$K^2 = \frac{2}{\langle I \rangle^2 T} \int_0^T \left(1 - \frac{\tau}{T}\right) \left\{ \langle I(t)I(t + \tau) \rangle - \langle I \rangle^2 \right\} d\tau = \frac{2}{T} \int_0^T \left(1 - \frac{\tau}{T}\right) \frac{\langle I(t)I(t + \tau) \rangle}{\langle I \rangle^2} - 1 d\tau \quad (2.4)$$

Though the speckle fluctuations are caused by electric field fluctuations, in practical set-ups the intensity fluctuations are measured. The normalized electric field autocorrelation function ($g_1(\tau)$) and the normalized intensity autocorrelation function ($g_2(\tau)$) are related through the Siegert relation [12]:

$$g_2(\tau) = 1 + \beta_M |g_1(\tau)|^2 \quad (2.5)$$

and are defined as:

$$g_1(\tau) = \frac{\langle E(t)E^*(t+\tau) \rangle_t}{\langle E(t)E^*(t) \rangle_t} \quad (2.6)$$

$$g_2(\tau) = \frac{\langle I(t)I(t+\tau) \rangle_t}{\langle I(t) \rangle_t^2} \quad (2.7)$$

Where β_M is a measurement-geometry specific constant [19], $E(t)$ represents the electric field at time t and $E^*(t)$ its complex conjugate. Finally, from equations (2.4)- (2.7) and the ergodicity principle we get the basic expression for K :

$$K(T) = \beta_M^{1/2} \left[\frac{2}{T} \int_0^T \left(1 - \frac{\tau}{T} \right) |g_1(\tau)|^2 d\tau \right]^{1/2} \quad (2.8)$$

The assumption that Eq. (2.8) is valid for ergodic systems implies that the time and ensemble average of the speckle pattern are equal and K can be quantified using σ_i and $\langle I \rangle$ from image pixels in time (subsequent frames) and in space. However, if a purely static component is present in the scattered electric field this component will produce a constant speckle contrast independent of camera exposure time and in addition, this component will have different temporal and spatial statistics (e.g. a temporal σ_i of zero). In many practical LSCI geometries the static component needs to be taken into account. By defining the electric field as a summation of the fluctuating (E_f) and the static (E_s) component: $E(t) = E_f(t) + E_s(t)$, a modified Siegert relation was proposed [36, 42]:

$$g_2(\tau) = 1 + \beta \left[\rho^2 |g_1(\tau)|^2 + 2\rho(1-\rho)|g_1(\tau)| + (1-\rho)^2 \right] \quad (2.9)$$

Which gives

$$K(T) = \beta_M^{1/2} \left(\frac{2}{T} \right)^{1/2} \left[\rho^2 \int_0^T \left(1 - \frac{\tau}{T} \right) |g_1(\tau)|^2 d\tau + 2\rho(1-\rho) \int_0^T \left(1 - \frac{\tau}{T} \right) |g_1(\tau)| d\tau + (1-\rho)^2 \right]^{1/2} \quad (2.10)$$

Where ρ is the fraction dynamically scattered light: $\rho = I_f / (I_f + I_s)$, with I_f the detected intensity of the fluctuating scattered light and I_s the detected intensity of the light scattered by static components. Parameters β_M and ρ depend on the measurement geometry and can be measured. To quantify the relation between K and blood flow dynamics an expression for the field ACF $g_1(\tau)$ is needed, which is parameterized by the characteristic decorrela-

tion time of the scattered electric field, τ_c . In LSCI it is conventional to assume a Lorentzian form [$g_1(\tau) = \exp(-(\tau/\tau_c))$] for Brownian motion and a Gaussian form [$g_1(\tau) = \exp(-(\tau/\tau_c)^2)$] for directional motion. Substituting the appropriate form of $g_1(\tau)$ in Eq. (2.10) results in an analytical expression of $K(T)$ from which τ_c can be derived. This analytical expression is given in Chapters 3 and 4 (Eq. (3.6), Lorentzian and Eq. (3.7)/Supplementary Eq. (4.10), Gaussian).

From the above it is clear that accurate estimation of β_M and ρ is important, as well as choosing an appropriate model for $g_1(\tau)$. Parthasarathy et al. [36] propose to use a multi-exposure speckle acquisition scheme to estimate β_M and ρ and τ_c accurately. It is commonly agreed that blood flow velocity and τ_c are inversely proportional to each other, but the proportionality constant of this relationship is topic of debate [24, 43], and *in vivo* quantification of the technique represents one of the challenges in LSCI. Since the integrated SDF-LSCI microcirculation imager can acquire raw speckle images and conventional SDF images of the same blood vessels, *in vivo* quantification is feasible. In Chapter 3 SDF-LSCI is explored using a multi-exposure acquisition scheme and assuming a Gaussian form of $g_1(\tau)$, for both an *in vitro* flow phantom and for the *in vivo* sublingual microcirculation. The relationship between $1/\tau_c$ and blood flow velocity is investigated, which gave interesting insight into the decorrelation by tissue dynamics relevant for LSCI. Another insufficiently explored area is the validity of the assumed forms of the ACF, often simply the Gaussian or Lorentzian form. In Chapter 4 $g_1(\tau)$ is revised within the theoretical frameworks of LDF and DWS, complemented by recent advances in the modelling of optical scattering of whole blood [44]. In addition, the influence of multiple scattering, a well-known bottleneck in LSCI (and also LDF) [45] is theoretically and experimentally assessed. The results are relevant to other dynamic light scattering flowmetry techniques for which the ability to accurately measure blood flow depends on the appropriateness of the assumed model for $g_1(\tau)$ and the accuracy in measuring $g_1(\tau)$, taking into account the optical properties of the scatterers and the geometry dependent multiple scattering in biological tissues. However, the acquisition simplicity, temporal and spatial measurement characteristics and automated analysis possibility of time-integrated speckle based methods (like LSCI) are advantageous for a non-invasive, compact, instantaneous and continuous microcirculation monitoring device.

2.5 REFERENCES

1. A. Lima and J. Bakker, "Noninvasive monitoring of peripheral perfusion," *Intensive Care Med.* 31, 1316-1326 (2005).
2. M. D. Stern, D. L. Lappe, P. D. Bowen, J. E. Chimosky, G. Holloway, H. Keiser, and R. Bowman, "Continuous measurement of tissue blood flow by laser-Doppler spectroscopy," *Am. J. Physiol.* 232, H441-H448 (1977).
3. W. Groner, J. W. Winkelman, A. G. Harris, C. Ince, G. J. Bouma, K. Messmer, and R. G. Nadeau, "Orthogonal polarization spectral imaging: a new method for study of the microcirculation," *Nat. Med.* 5, 1209-1212 (1999).
4. A. Jaap, C. Pym, C. Seamark, A. Shore, and J. Tooke, "Microvascular Function in Type 2 (Non-insulin-dependent) Diabetes: Improved Vasodilation After One Year of Good Glycaemic Control," *Diabet. Med.* 12, 1086-1091 (1995).
5. M. Roustit and J.-L. Cracowski, "Non-invasive Assessment of Skin Microvascular Function in Humans: An Insight Into Methods," *Microcirculation* 19, 47-64 (2012).
6. K.-D. Schaser, U. Settmacher, G. Puhl, L. Zhang, T. Mittlmeier, J. Stover, B. Vollmar, M. Menger, P. Neuhaus, and N. Haas, "Noninvasive analysis of conjunctival microcirculation during carotid artery surgery reveals microvascular evidence of collateral compensation and stenosis-dependent adaptation," *J. Vasc. Surg.* 37, 789-797 (2003).
7. W. D. Strain, D. D. Adingupu, and A. C. Shore, "Microcirculation on a large scale: techniques, tactics and relevance of studying the microcirculation in larger population samples," *Microcirculation* 19, 37-46 (2011).
8. K. R. Mathura, G. J. Bouma, and C. Ince, "Abnormal microcirculation in brain tumours during surgery," *The Lancet* 358, 1698-1699 (2001).
9. D. De Backer, S. Hollenberg, C. Boerma, P. Goedhart, G. Büchele, G. Ospina-Tascon, I. Dobbe, and C. Ince, "How to evaluate the microcirculation: report of a round table conference," *Crit. Care* 11 (2007).
10. J. G. Dobbe, G. J. Streekstra, B. Atasever, R. Van Zijderveld, and C. Ince, "Measurement of functional microcirculatory geometry and velocity distributions using automated image analysis," *Med. Biol. Eng. Comput.* 46, 659-670 (2008).
11. J. Hecht, "Short history of laser development," *Optical Engineering* 49 (2010).
12. B. J. Berne and R. Pecora, *Dynamic light scattering: with applications to chemistry, biology, and physics* (Courier Dover Publications, 2000).
13. M. Stern, "In vivo evaluation of microcirculation by coherent light scattering," *Nature* 254, 56-58 (1975).
14. A. Fercher and J. Briers, "Flow visualization by means of single-exposure speckle photography," *Opt. Commun.* 37, 326-330 (1981).
15. D. Pine, D. Weitz, P. Chaikin, and E. Herbolzheimer, "Diffusing wave spectroscopy," *Phys. Rev. Lett.* 60, 1134 (1988).
16. P. Vennemann, R. Lindken, and J. Westerweel, "In vivo whole-field blood velocity measurement techniques," *Experiments in fluids* 42, 495-511 (2007).
17. J. D. Briers, "Laser Doppler, speckle and related techniques for blood perfusion mapping and imaging," *Physiol. Meas.* 22, R35 (2001).
18. Y. Aizu and T. Asakura, "Coherent optical techniques for diagnostics of retinal blood flow," *J. Biomed. Opt.* 4, 61-75 (1999).
19. J. W. Goodman, *Speckle phenomena in optics: theory and applications* (Roberts and Company Publishers, Greenwood Village, CO, 2007).
20. R. Bonner and R. Nossal, "Model for laser Doppler measurements of blood flow in tissue," *Appl. Opt.* 20, 2097-2107 (1981).
21. O. B. Thompson and M. K. Andrews, "Tissue perfusion measurements: multiple-exposure laser speckle analysis generates laser Doppler-like spectra," *J. Biomed. Opt.* 15 (2010).
22. V. V. Tuchin, *Tissue optics: light scattering methods and instruments for medical diagnosis* (SPIE press Bellingham, 2007)
23. J. D. Briers, "Laser Doppler and time-varying speckle: a reconciliation," *JOSA A* 13, 345-350 (1996).
24. M. J. Draijer, E. Hondebrink, M. Larsson, T. G. van Leeuwen, and W. Steenbergen, "Relation between the contrast in time integrated dynamic speckle patterns and the power spectral density of their temporal intensity fluctuations," *Opt. Express* 18 (2010).
25. D. Weitz, J. Zhu, D. Durian, H. Gang, and D. Pine,

- "Diffusing-wave spectroscopy: The technique and some applications," *Phys. Scr.* 1993, 610 (1993).
26. G. Dietsche, M. Ninck, C. Ortoft, J. Li, F. Jailon, and T. Gisler, "Fiber-based multispeckle detection for time-resolved diffusing-wave spectroscopy: characterization and application to blood flow detection in deep tissue," *Appl. Opt.* 46, 8506-8514 (2007).
 27. J. D. Briers and S. Webster, "Laser speckle contrast analysis (LASCA): a non-scanning, full-field technique for monitoring capillary blood flow," *J. Biomed. Opt.* 1, 174-179 (1996).
 28. T. M. Le, J. Paul, and S. Ong, "Laser speckle imaging for blood flow analysis," in *Computational Biology* (Springer, 2010), pp. 243-271.
 29. H. Cheng, Q. Luo, Q. Liu, Q. Lu, H. Gong, and S. Zeng, "Laser speckle imaging of blood flow in microcirculation," *Phys. Med. Biol.* 49, 1347 (2004).
 30. P. Zakharov, A. Völker, A. Buck, B. Weber, and F. Scheffold, "Quantitative modeling of laser speckle imaging," *Opt. Lett.* 31, 3465-3467 (2006).
 31. S. J. Kirkpatrick, D. D. Duncan, and E. M. Wells-Gray, "Detrimental effects of speckle-pixel size matching in laser speckle contrast imaging," *Opt. Lett.* 33, 2886-2888 (2008).
 32. S. Yuan, A. Devor, D. A. Boas, and A. K. Dunn, "Determination of optimal exposure time for imaging of blood flow changes with laser speckle contrast imaging," *Appl. Opt.* 44, 1823-1830 (2005).
 33. D. Zhu, W. Lu, Y. Weng, H. Cui, and Q. Luo, "Monitoring thermal-induced changes in tumor blood flow and microvessels with laser speckle contrast imaging," *Appl. Opt.* 46, 1911-1917 (2007).
 34. Z. Wang, S. Hughes, S. Dayasundara, and R. S. Menon, "Theoretical and experimental optimization of laser speckle contrast imaging for high specificity to brain microcirculation," *J. Cereb. Blood Flow Metab.* 27, 258-269 (2006).
 35. R. Bandyopadhyay, A. Gittings, S. Suh, P. Dixon, and D. Durian, "Speckle-visibility spectroscopy: A tool to study time-varying dynamics," *Rev. Sci. Instrum.* 76 (2005).
 36. A. B. Parthasarathy, W. J. Tom, A. Gopal, X. Zhang, and A. K. Dunn, "Robust flow measurement with multi-exposure speckle imaging," *Opt. Express* 16, 1975-1989 (2008).
 37. C. Cheung, J. P. Culver, K. Takahashi, J. H. Greenberg, and A. Yodh, "In vivo cerebrovascular measurement combining diffuse near-infrared absorption and correlation spectroscopies," *Phys. Med. Biol.* 46, 2053 (2001).
 38. M. Ninck, M. Untenberger, and T. Gisler, "Diffusing-wave spectroscopy with dynamic contrast variation: disentangling the effects of blood flow and extravascular tissue shearing on signals from deep tissue," *Biomedical optics express* 1, 1502-1513 (2010).
 39. K. Johansson, H. Ahn, J. Lindhagen, and O. Lundgren, "Tissue penetration and measuring depth of laser Doppler flowmetry in the gastrointestinal application," *Scand. J. Gastroenterol.* 22, 1081-1088 (1987).
 40. M. Draijer, E. Hondebrink, T. Van Leeuwen, and W. Steenbergen, "Review of laser speckle contrast techniques for visualizing tissue perfusion," *Lasers Med. Sci.* 24, 639-651 (2009).
 41. P. Li, S. Ni, L. Zhang, S. Zeng, and Q. Luo, "Imaging cerebral blood flow through the intact rat skull with temporal laser speckle imaging," *Opt. Lett.* 31, 1824-1826 (2006).
 42. D. A. Boas and A. K. Dunn, "Laser speckle contrast imaging in biomedical optics," *J. Biomed. Opt.* 15, 011109-011109-011112 (2010).
 43. D. D. Duncan and S. J. Kirkpatrick, "Can laser speckle flowmetry be made a quantitative tool?," *JOSA A* 25, 2088-2094 (2008).
 44. N. Bosschaart, G. J. Edelman, M. C. Aalders, T. G. van Leeuwen, and D. J. Faber, "A literature review and novel theoretical approach on the optical properties of whole blood," *Lasers Med. Sci.* 29, 453-479 (2014).
 45. D. Briers, D. D. Duncan, E. Hirst, S. J. Kirkpatrick, M. Larsson, W. Steenbergen, T. Stromberg, and O. B. Thompson, "Laser speckle contrast imaging: theoretical and practical limitations," *J. Biomed. Opt.* 18, 066018-066018 (2013)